Supplementary Information

Discovery of a New Inhibitor for the YTH Domain-containing m^{6}A RNA Readers

Chuan-Hui Wang, Huiqing Zhou*

Department of Chemistry, Merkert Chemistry Center, Boston College, Chestnut Hill, MA 02467, USA

*To whom correspondence should be addressed.

Email: zhouaf@bc.edu

Characterization of the commercial N-7 compound.

We characterized the commercial **N-7** via LC-MS and ^{1}H NMR spectroscopy (Fig. S4, ESI†). LC-MS results show a single peak in the LC trace and MS measured the expected mass of the **N-7** compound (measured ion mass $[M + H]^{+}$ = 373.18; calculated molecular weight of **N-7** [M] = 372.19). ^{1}H NMR shows characteristic ^{1}H resonances for **N-7** compound: ^{1}H NMR (500 MHZ, DMSO-d6) δ (ppm): 8.25 (1H, s), 8.17 (1H, s), 7,64 (1H, s), 4.97-4.92 (1H, m), 4.11-4.02 (2H, m), 3.68 (2H, m), 3.48 (2H, s), 3.41 (2H, s), 3.23-3.19 (2H, m), 3.09-2.94 (1H, m), 2.43-2.39 (2H, m), 2.31-2.27 (2H, m), 2.24-2.23 (2H, m), 2.02-1.94 (2H, m) (Fig. S4, ESI†).

Supplementary Figures

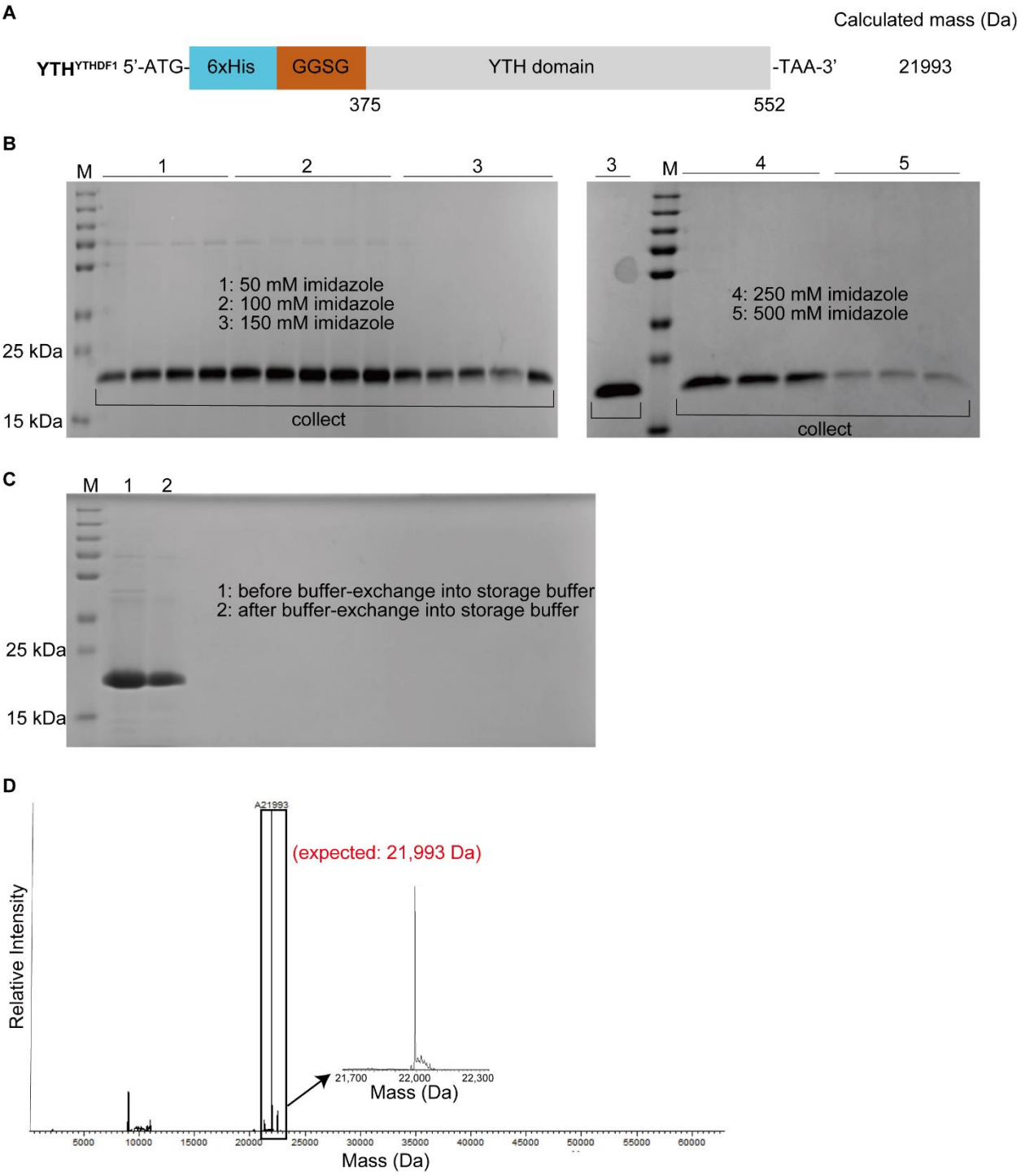

Fig. S1. Purify and characterize YTH^{YTHDF1} protein. (**A**) The DNA sequence information of YTH^{YTHDF1}. (**B**) SDS-PAGE characterizations of the purified YTH^{YTHDF1} protein.

YTH^{YTHDF1} protein was purified by a Nickel column with an imidazole concentration gradient in lysis buffer. (**C**) SDS-PAGE characterizations of the purity of YTH^{YTHDF1} protein before and after buffer exchange. This is the raw gel data for **Fig. 1B**. (**D**) Full deconvolution of MS data of YTH^{YTHDF1} protein (black, observed mass; red, theoretical mass) and zoom-in data are shown in **Fig. 1B**.

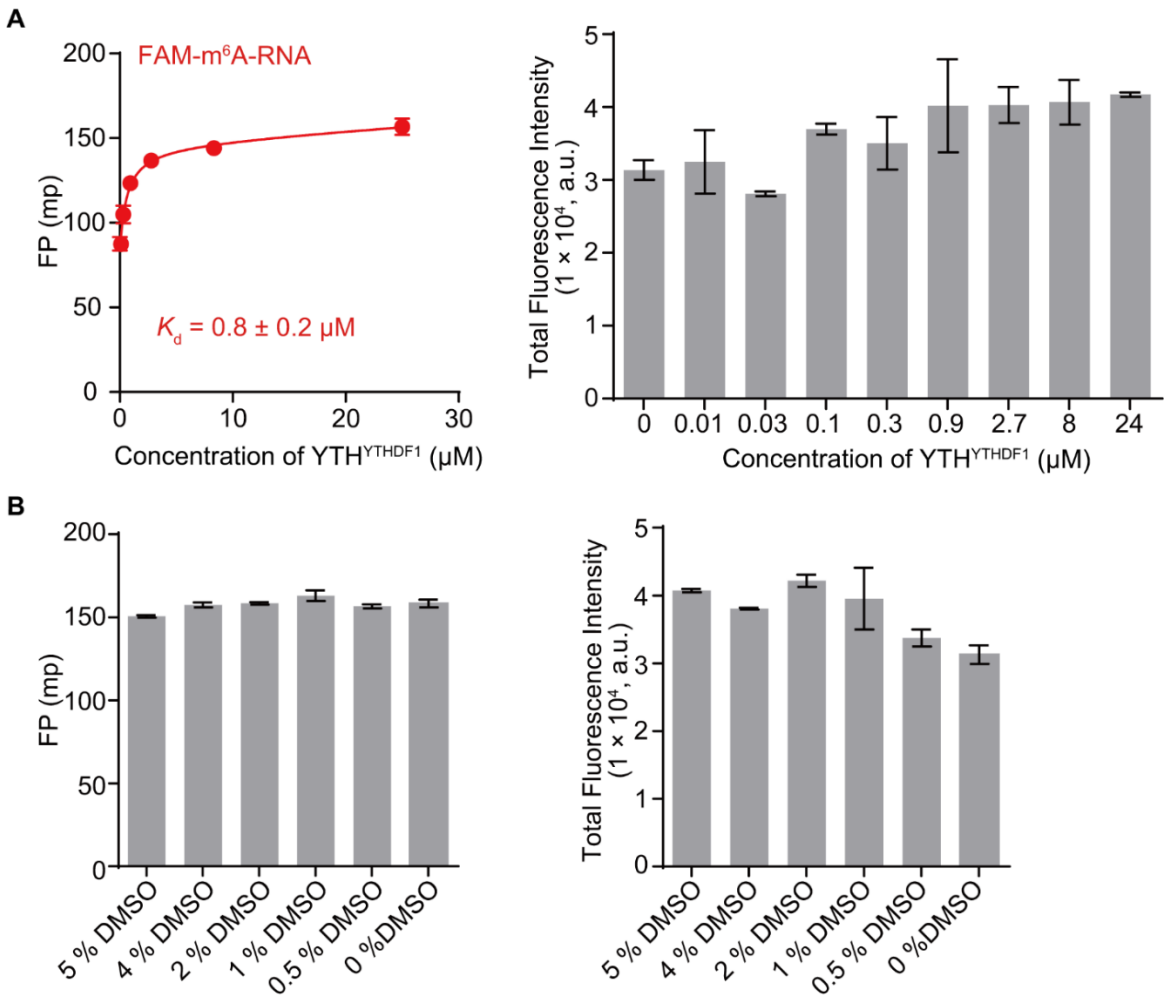

Fig. S2. Setup for FP competition assay screening. (A) Compare the changing of total fluorescence intensity during the titration of the purified YTH^{YTHDF1} by FAM-m^{6}A-RNA in the FP binding assay as the concentration of YTH^{YTHDF1} proteins increases. Part of the data is shown in **Fig. 1D**. Data are presented as mean ± standard deviation (SD) with n=3 biological replicates. (**B**) Shown is the displacement of FAM-m^{6}A-RNA from YTH^{YTHDF1} by DMSO by the FP competition assay. Data are presented as mean ± SD with n=2 biological replicates and up to 5% DMSO does not affect the FP signal and total fluorescence intensity of FAM-m^{6}A-RNA.

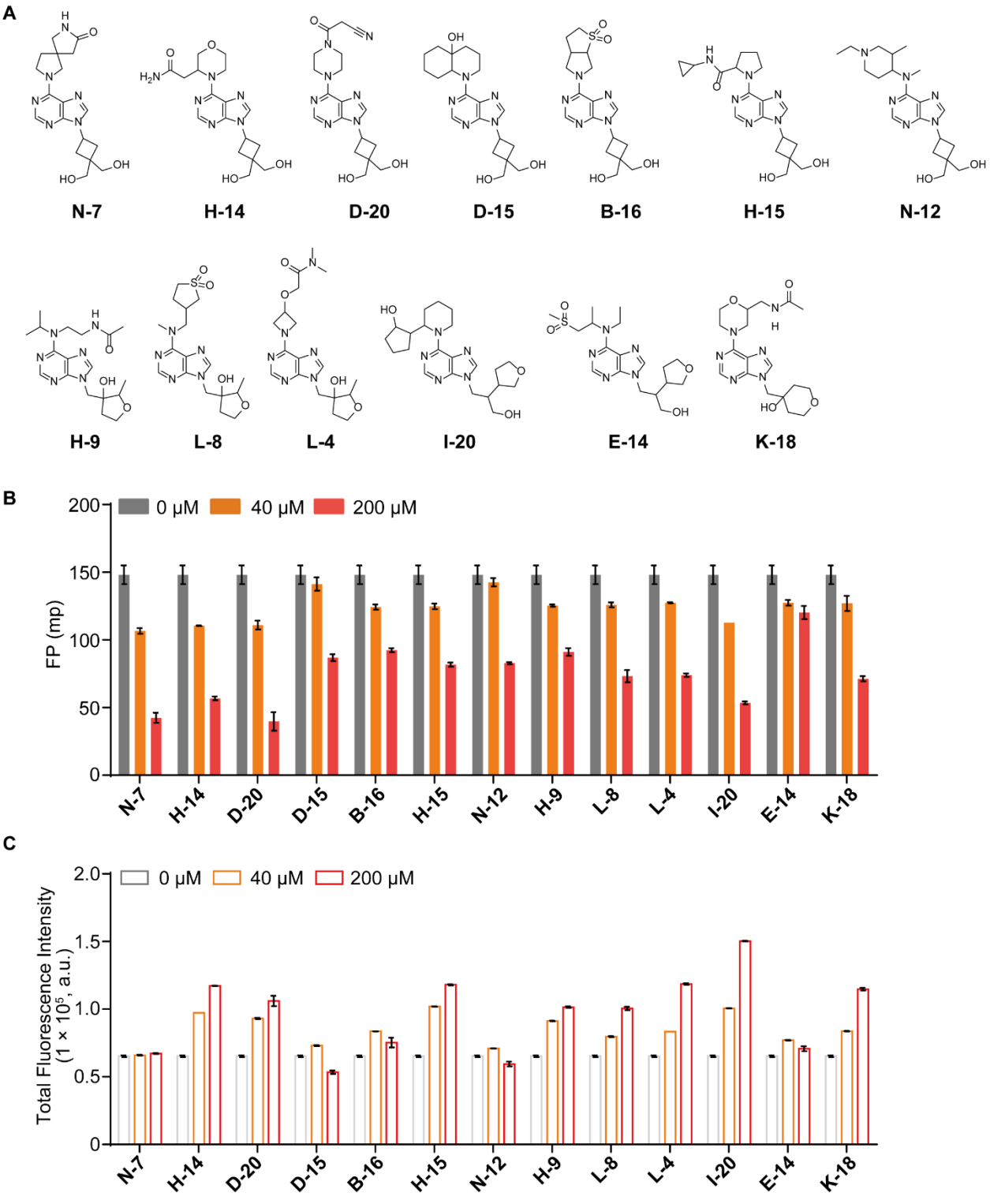

Fig. S3. Dose-response testing of potential screening hits. (**A**) The chemical structures of hit compounds. (**B**) Shown is the displacement of FAM-m^{6}A-RNA from

YTH^{YTHDF1} by DMSO or hit compounds (40 μM and 200 μM) by the FP competition assay. Data are presented as mean ± SD with n=2 technical replicates. (**C**) Compare the changing of total fluorescence intensity during displacement of FAM-m^6A-RNA from YTH^{YTHDF1} by DMSO or hit compounds (40 μM and 200 μM) by the FP competition assay. Data are presented as mean ± SD with n=2 technical replicates.

LC-MS spectra of **N-7**

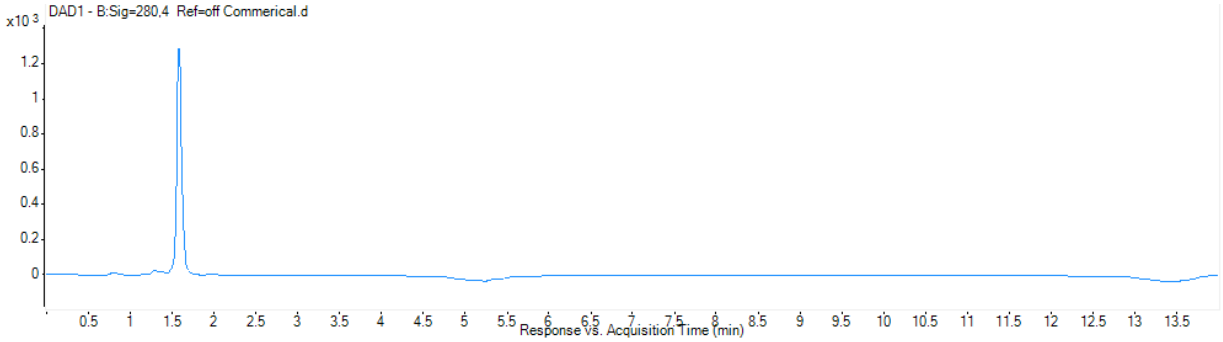

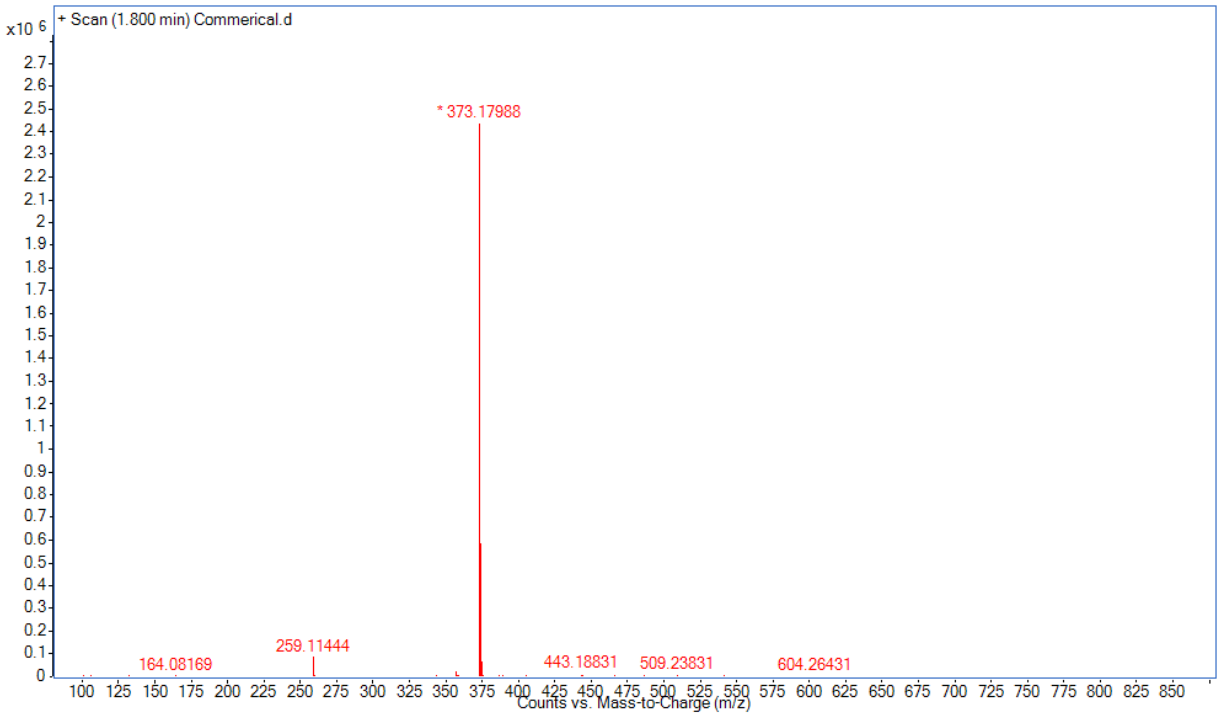

^{1}H NMR spectra of **N-7**

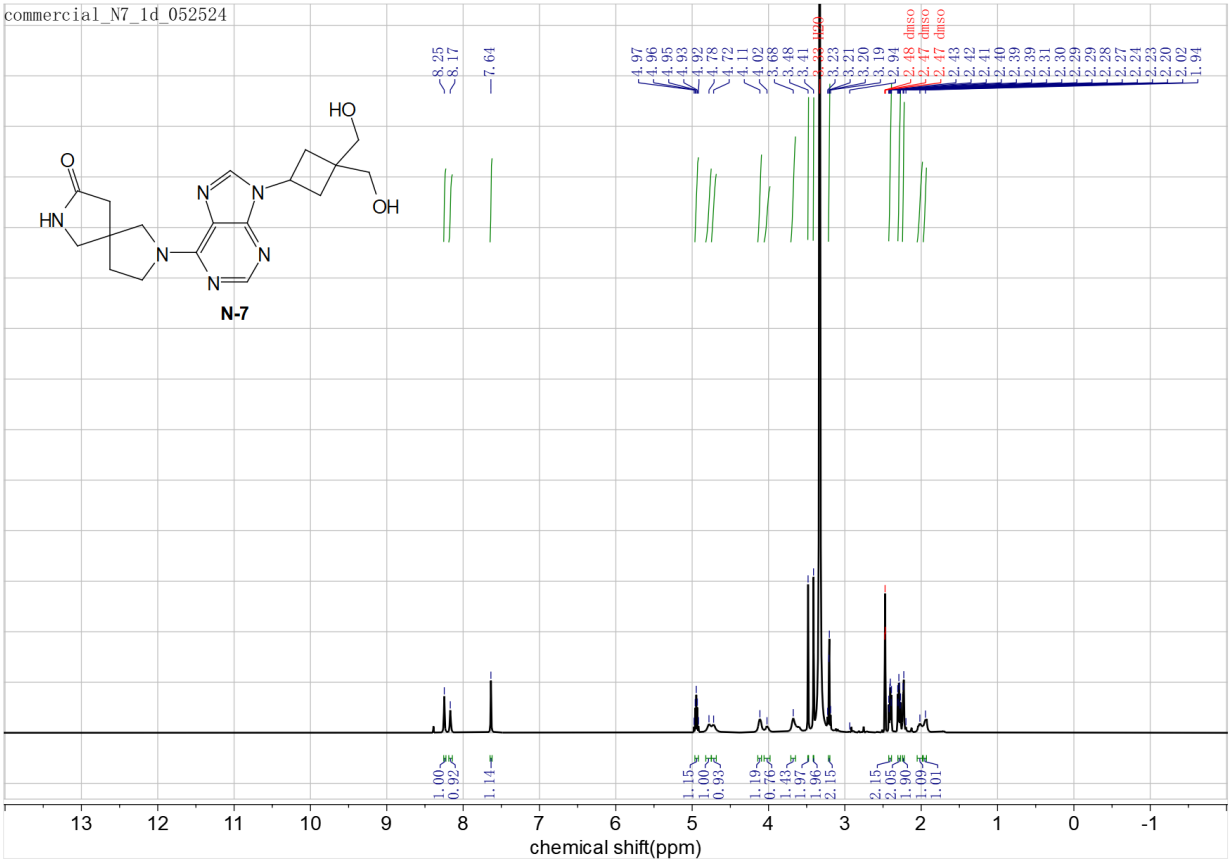

Fig. S4. LC-MS and ^{1}H NMR spectra for the N-7 compound purchased from Enamine Inc.

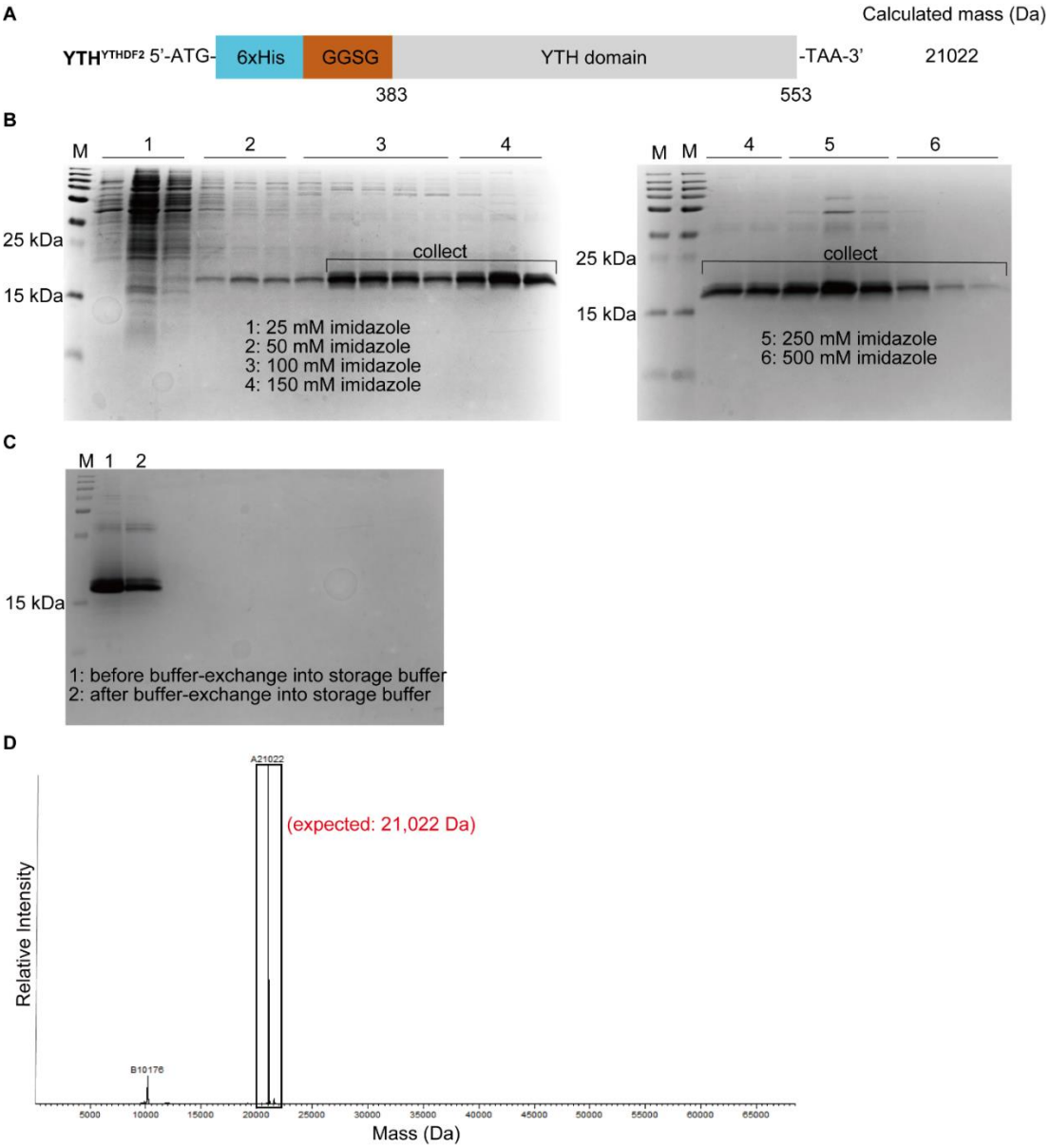

Fig. S5. Purify and characterize YTH^{YTHDF2} protein. (**A**) The DNA sequence information of YTH^{YTHDF2}. (**B**) SDS-PAGE characterizations of the purified YTH^{YTHDF2} protein. YTH^{YTHDF2} protein was purified by a Nickel column with an imidazole concentration gradient in lysis buffer. (**C**) SDS-PAGE characterizations of the purity of YTH^{YTHDF2} protein before and after buffer exchange. (**D**) Full deconvolution of MS data of YTH^{YTHDF2} protein (black, observed mass; red, theoretical mass).

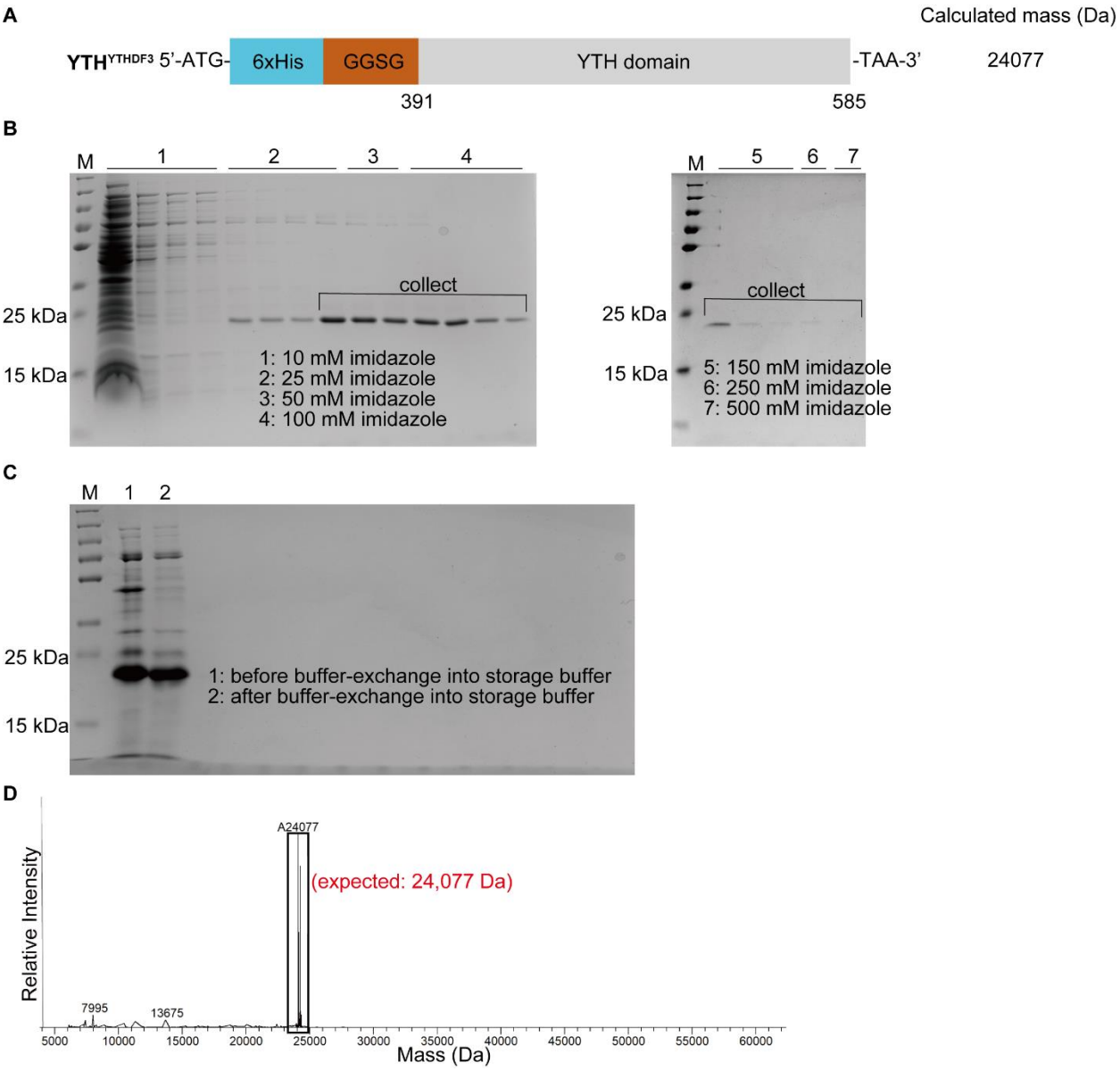

Fig. S6. Purify and characterize YTH^{YTHDF3} protein. (**A**) The DNA sequence information of YTH^{YTHDF3}. (**B**) SDS-PAGE characterizations of the purified YTH^{YTHDF3} protein. YTH^{YTHDF3} protein was purified by a Nickel column with an imidazole concentration gradient in lysis buffer. (**C**) SDS-PAGE characterizations of the purity of YTH^{YTHDF3} protein before and after buffer exchange. (**D**) Full deconvolution of MS data of YTH^{YTHDF3} protein (black, observed mass; red, theoretical mass).

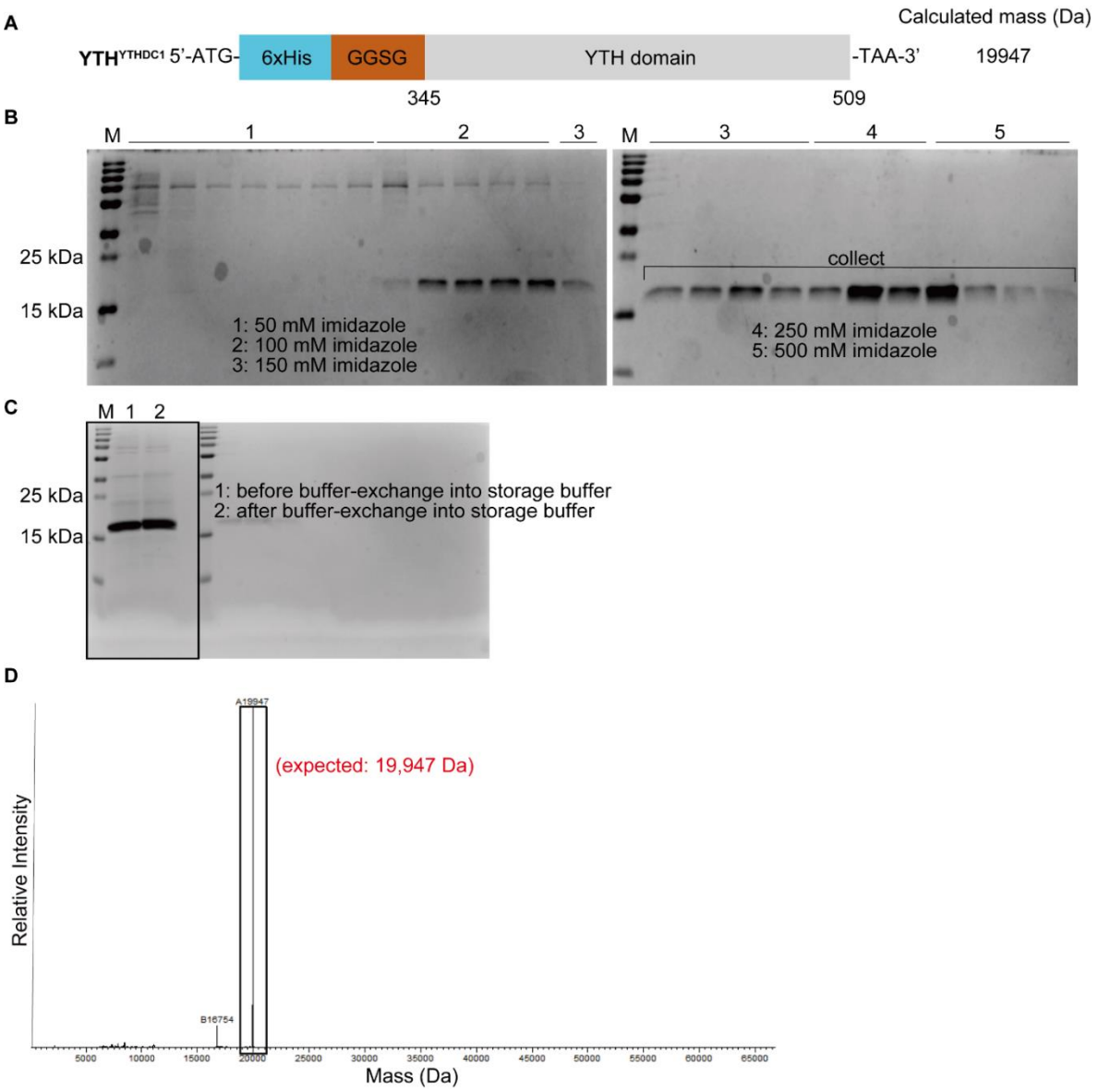

Fig. S7. Purify and characterize YTH^{YTHDC1} protein. (**A**) The DNA sequence information of YTH^{YTHDC1}. (**B**) SDS-PAGE characterizations of the purified YTH^{YTHDC1} protein. YTH^{YTHDC1} protein was purified by a Nickel column with an imidazole concentration gradient in lysis buffer. (**C**) SDS-PAGE characterizations of the purity of YTH^{YTHDC1} protein before and after buffer exchange. (**D**) Full deconvolution of MS data of YTH^{YTHDC1} protein (black, observed mass; red, theoretical mass).

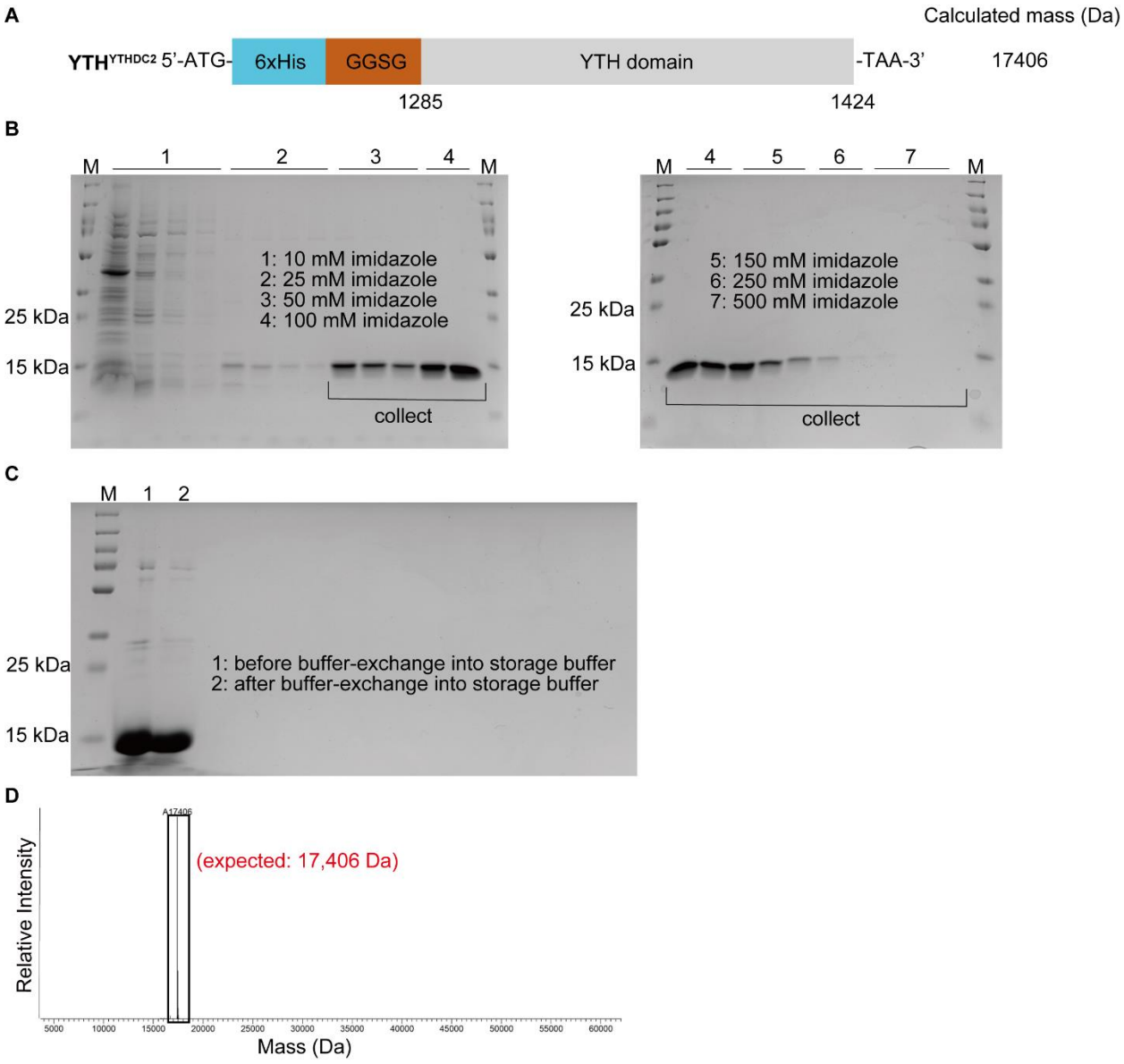

Fig. S8. Purify and characterize YTH^{YTHDC2} protein. (**A**) The DNA sequence information of YTH^{YTHDC2}. (**B**) SDS-PAGE characterizations of the purified YTH^{YTHDC2} protein. YTH^{YTHDC2} protein was purified by a Nickel column with an imidazole concentration gradient in lysis buffer. (**C**) SDS-PAGE characterizations of the purity of YTH^{YTHDC2} protein before and after buffer exchange. (**D**) Full deconvolution of MS data of YTH^{YTHDC2} protein (black, observed mass; red, theoretical mass).

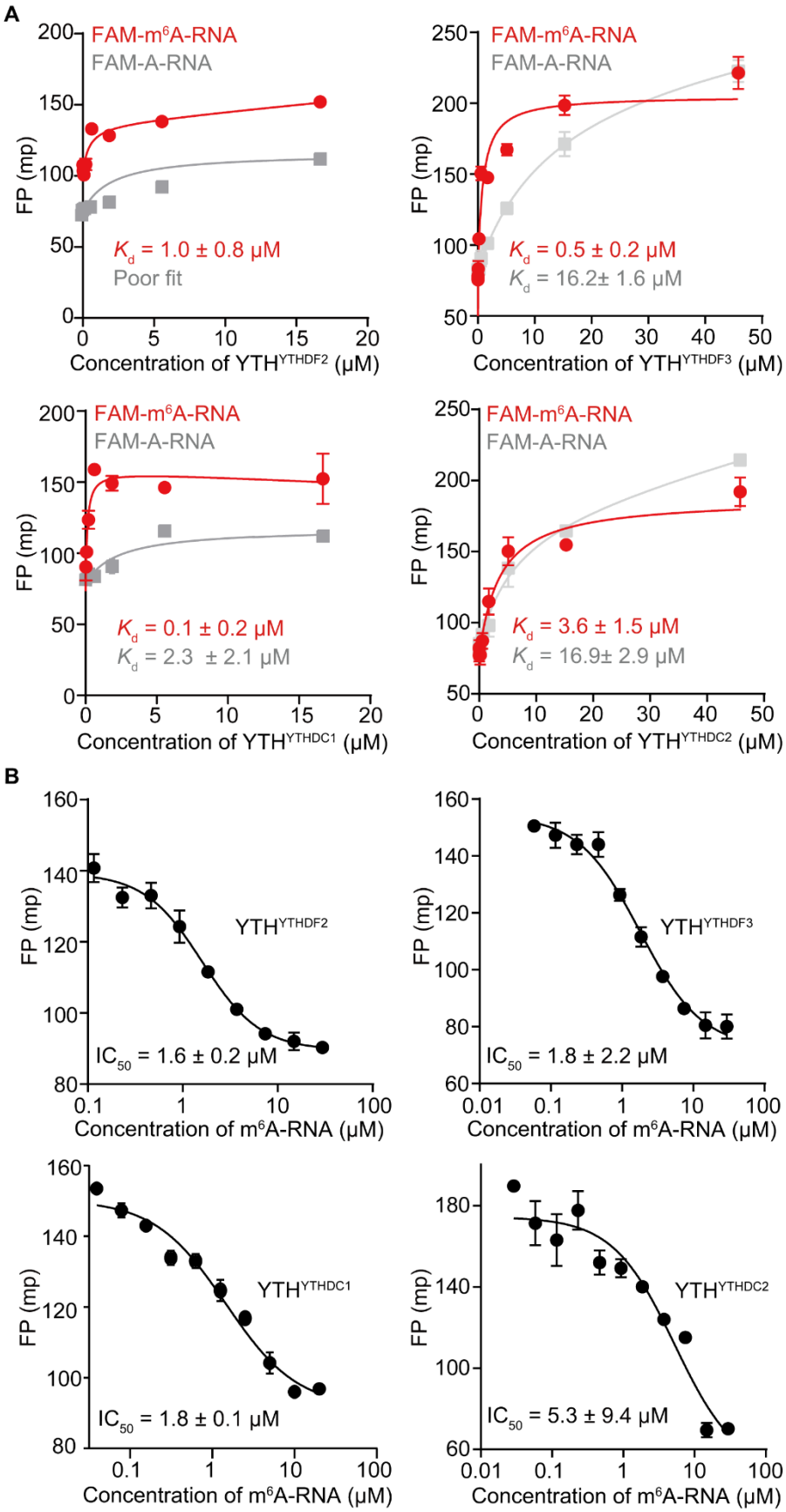
A
FAM-m6A-RNA
FAM-A-RNA
FP (mp)
Kd = 1.0 ± 0.8 μM
Poor fit
Concentration of YTHYTHDF2 (μM)
Kd = 0.5 ± 0.2 μM
Kd = 16.2± 1.6 μM
Concentration of YTHYTHDF3 (μM)
Kd = 0.1 ± 0.2 μM
Kd = 2.3 ± 2.1 μM
Concentration of YTHYTHDC1 (μM)
Kd = 3.6 ± 1.5 μM
Kd = 16.9± 2.9 μM
Concentration of YTHYTHDC2 (μM)
B
YTHYTHDF2
IC50 = 1.6 ± 0.2 μM
Concentration of m6A-RNA (μM)
YTHYTHDF3
IC50 = 1.8 ± 2.2 μM
YTHYTHDC1
IC50 = 1.8 ± 0.1 μM
YTHYTHDC2
IC50 = 5.3 ± 9.4 μM

Fig. S9. Confirm the purified YTH^{YTHDF2}, YTH^{YTHDF3}, YTH^{YTHDC1}, and YTH^{YTHDC2} proteins as m^{6}A readers by the FP assay. (**A**) Shown are FP binding data and fitted binding curves for YTH-domain proteins and FAM-m^{6}A-RNA or FAM-A-RNA. Data are presented as mean ± SD with n=2 or 3 biological replicates. (**B**) Shown is the displacement of FAM-m^{6}A-RNA from YTH-domain proteins by the non-fluorescent m^{6}A-RNA by the FP competition assay with the fitted IC_{50} value. Data are presented as mean ± SD with n=3 biological replicates.

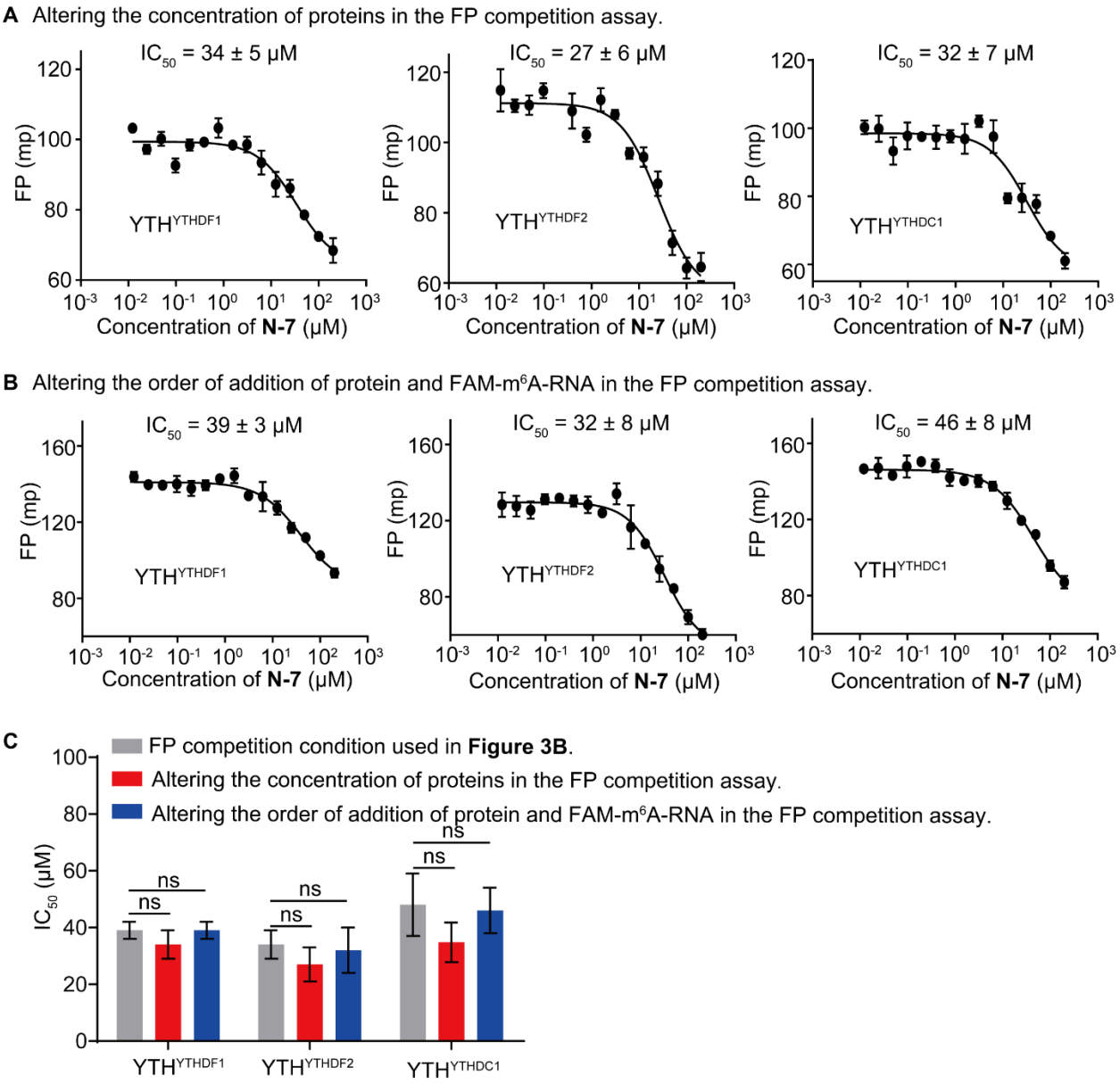

Fig. S10. N-7 is a *pan*-YTH domain inhibitor. (**A**) Dose-response curves of the FP competition assay using compound **N-7** against 0.8 μM YTH^{YTHDF1}, 1.0 μM YTH^{YTHDF2}, and 0.1 μM YTH^{YTHDC1} proteins, respectively. Data are presented as mean ± SD with n=3 biological replicates. (**B**) Dose-response curves of the FP competition assay using FAM-m^{6}A-RNA against different concentrations of **N-7** and YTH^{YTHDF1}, YTH^{YTHDF2}, or

YTH^{YTHDC1} proteins complex. Data are presented as mean ± SD with n=3 biological replicates. (**C**) IC_{50} values of **N-7** exhibited no significant changes under different FP competition assay conditions. The two-tailed *t*-test was used to assess the statistical significance of the difference between the two samples, with the *p*-value indicated as “ns” for $p \geq 0.05$.

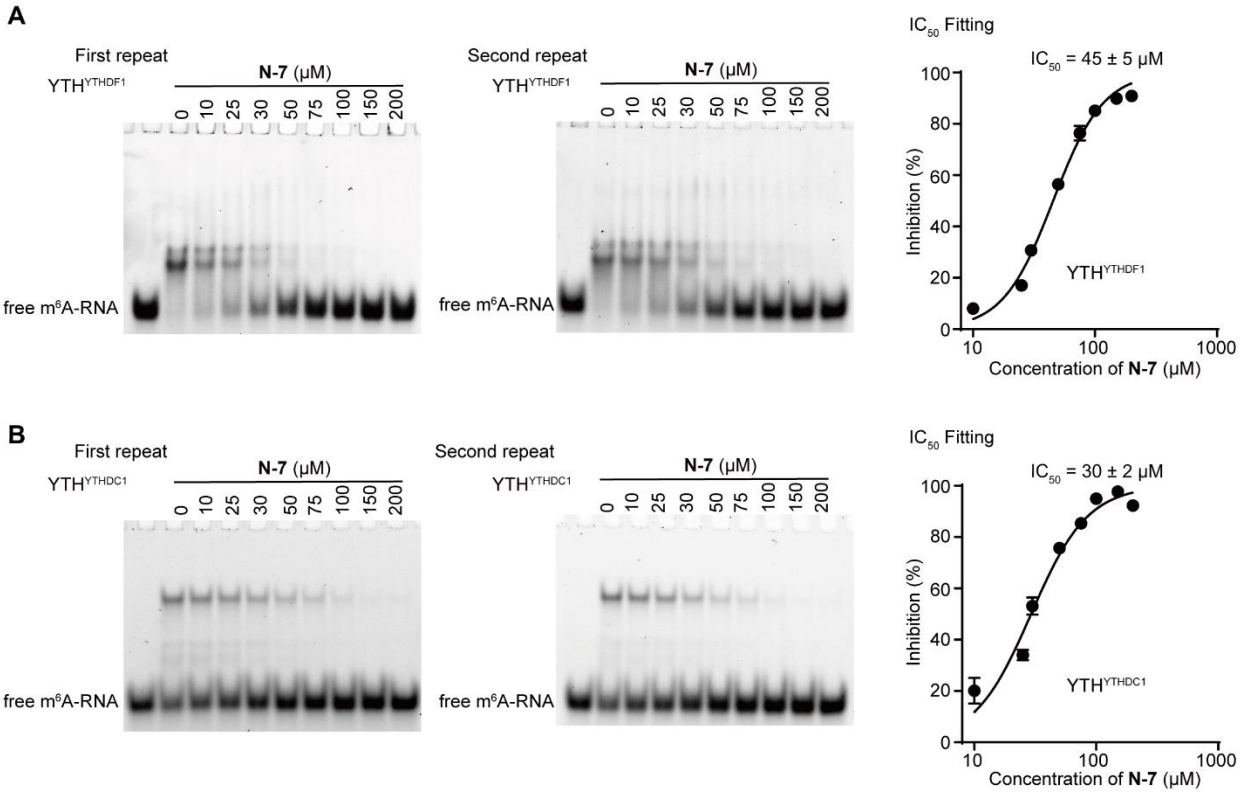

Fig. S11. N-7 demonstrated inhibition of the YTH domain proteins-RNA complex formation. (**A**) RNA electrophoretic mobility shift assay (REMSA) shows **N-7**'s inhibitory effect on the RNA-binding activity of YTH^{YTHDF1} (left), with quantification of IC_{50} values for **N-7** inhibition of YTH^{YTHDF1} (right). (**B**) REMSA shows **N-7**'s inhibitory effect on the RNA-binding activity of YTH^{YTHDC1} (left), with quantification of IC_{50} values for **N-7** inhibition of YTH^{YTHDC1} (right).

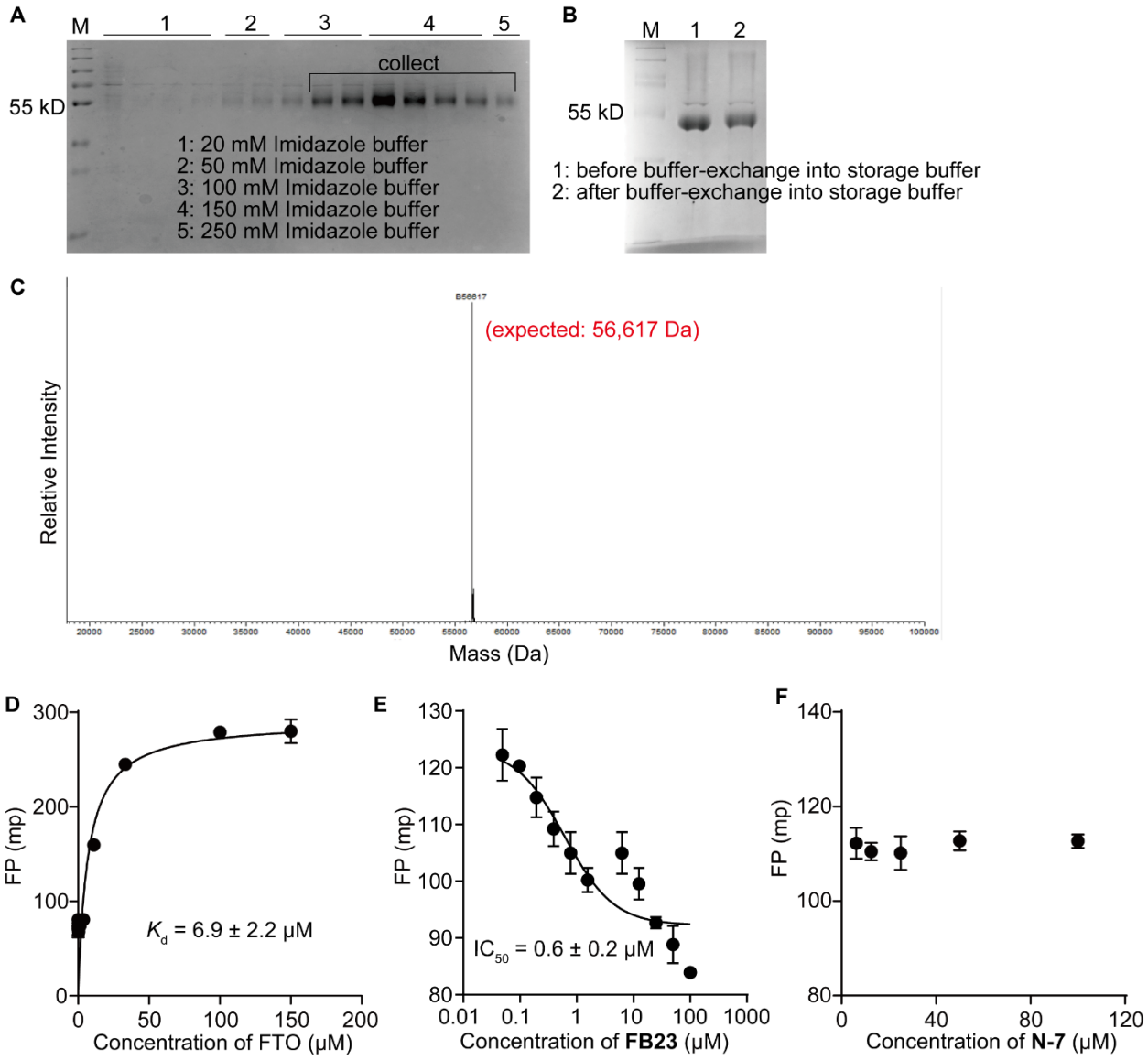

Fig. S12. Purify and characterize FTO protein. (**A**) SDS-PAGE characterizations of the purified FTO protein. FTO protein was purified by a Nickel column with an imidazole concentration gradient in lysis buffer. (**B**) SDS-PAGE characterizations of the purity of FTO protein before and after buffer exchange. (**C**) Full deconvolution of MS data of FTO protein (black, observed mass; red, theoretical mass). (**D**) Shown are FP binding data and fitted binding curves for FTO and FAM-m^{6}A-RNA. Data are presented as mean ± SD

with n=3 biological replicates. (**E**) Dose-response curves of the FP competition assay using compound **FB23** against FTO protein. Data are presented as mean ± SD with n=3 biological replicates. (**F**) Dose-response curves of the FP competition assay using compound **N-7** against FTO protein. Data are presented as mean ± SD with n=3 biological replicates.

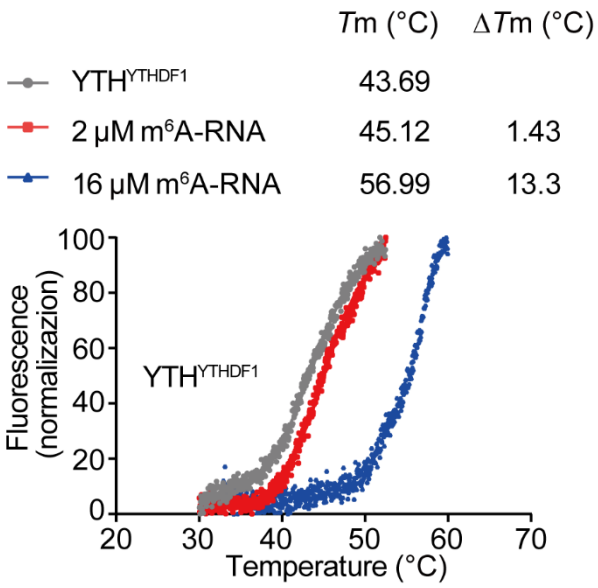

Fig. S13. Thermal shift assays were performed on the YTH^{YTHDF1} protein in the presence of m^{6}A-RNA.

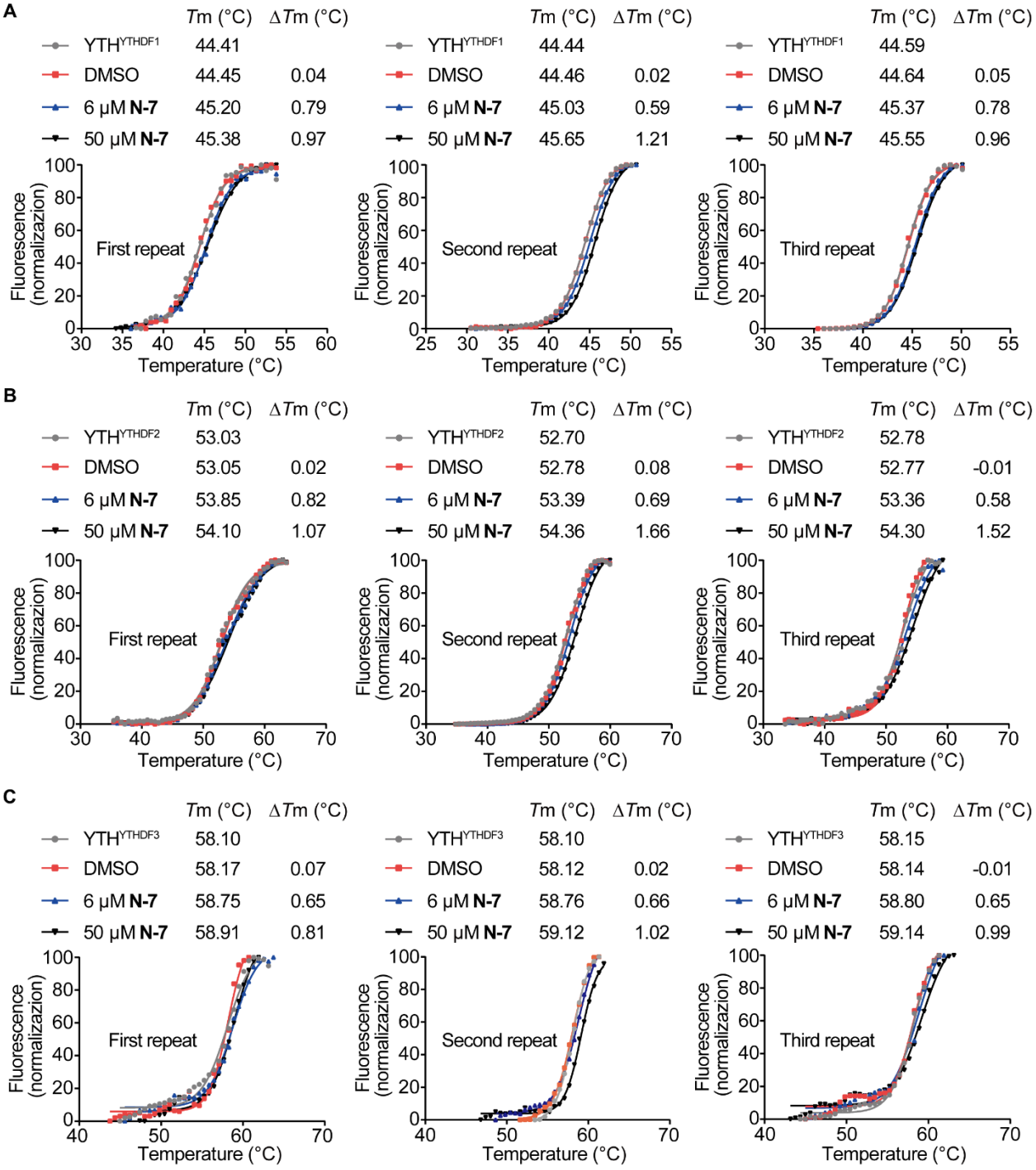
A
Tm (°C) ΔTm (°C)
YTH^YTHDF1 44.41
DMSO 44.45 0.04
6 μM N-7 45.20 0.79
50 μM N-7 45.38 0.97
Tm (°C) ΔTm (°C)
YTH^YTHDF1 44.44
DMSO 44.46 0.02
6 μM N-7 45.03 0.59
50 μM N-7 45.65 1.21
Tm (°C) ΔTm (°C)
YTH^YTHDF1 44.59
DMSO 44.64 0.05
6 μM N-7 45.37 0.78
50 μM N-7 45.55 0.96
First repeat
Second repeat
Third repeat
Fluorescence (normalizazion)
Temperature (°C)
B
Tm (°C) ΔTm (°C)
YTH^YTHDF2 53.03
DMSO 53.05 0.02
6 μM N-7 53.85 0.82
50 μM N-7 54.10 1.07
Tm (°C) ΔTm (°C)
YTH^YTHDF2 52.70
DMSO 52.78 0.08
6 μM N-7 53.39 0.69
50 μM N-7 54.36 1.66
Tm (°C) ΔTm (°C)
YTH^YTHDF2 52.78
DMSO 52.77 -0.01
6 μM N-7 53.36 0.58
50 μM N-7 54.30 1.52
First repeat
Second repeat
Third repeat
Fluorescence (normalizazion)
Temperature (°C)
C
Tm (°C) ΔTm (°C)
YTH^YTHDF3 58.10
DMSO 58.17 0.07
6 μM N-7 58.75 0.65
50 μM N-7 58.91 0.81
Tm (°C) ΔTm (°C)
YTH^YTHDF3 58.10
DMSO 58.12 0.02
6 μM N-7 58.76 0.66
50 μM N-7 59.12 1.02
Tm (°C) ΔTm (°C)
YTH^YTHDF3 58.15
DMSO 58.14 -0.01
6 μM N-7 58.80 0.65
50 μM N-7 59.14 0.99
First repeat
Second repeat
Third repeat
Fluorescence (normalizazion)
Temperature (°C)

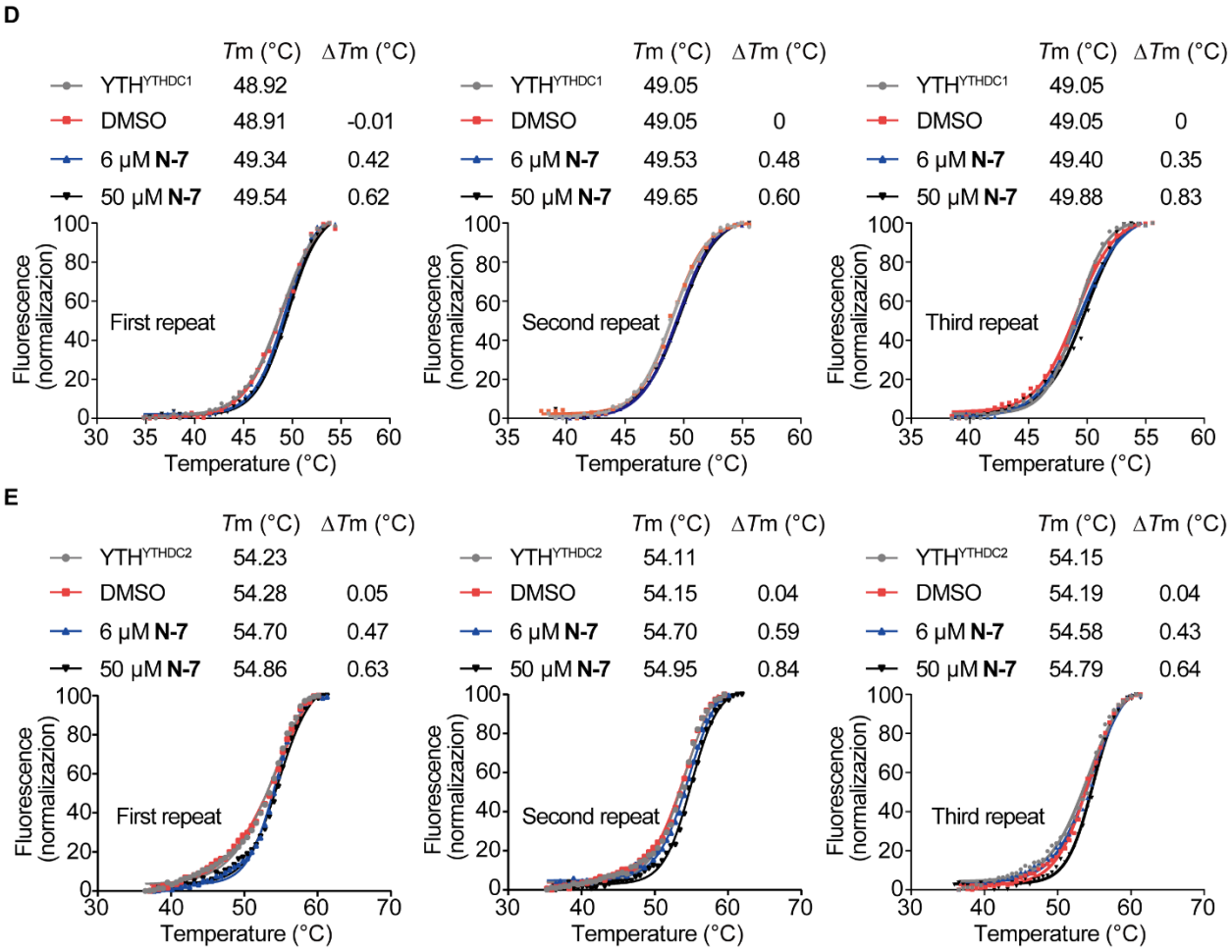

Fig. S14. Thermal shift assays results for the stabilization effect of N-7 against five YTH-domain proteins, including YTH^{YTHDF1} (A), YTH^{YTHDF2} (B), YTH^{YTHDF3} (C), YTH^{YTHDC1} (D), and YTH^{YTHDC2} (E). This figure provides the raw data for the plot shown in **Fig. 4B**.

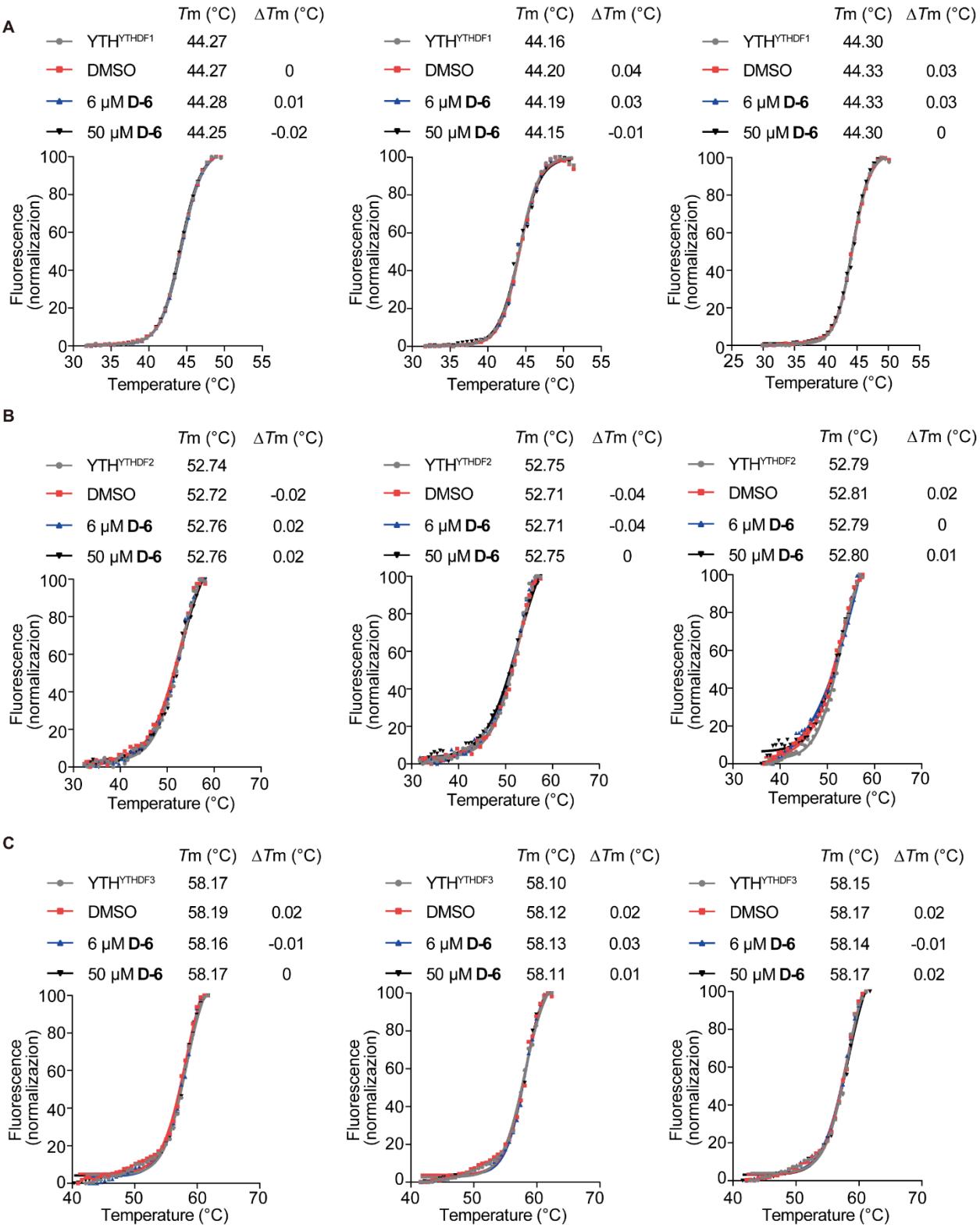
A
Tm (°C) ΔTm (°C)
YTH^YTHDF1 44.27
DMSO 44.27 0
6 μM D-6 44.28 0.01
50 μM D-6 44.25 -0.02
Tm (°C) ΔTm (°C)
YTH^YTHDF1 44.16
DMSO 44.20 0.04
6 μM D-6 44.19 0.03
50 μM D-6 44.15 -0.01
Tm (°C) ΔTm (°C)
YTH^YTHDF1 44.30
DMSO 44.33 0.03
6 μM D-6 44.33 0.03
50 μM D-6 44.30 0
Fluorescence (normalizazion)
Temperature (°C)
B
Tm (°C) ΔTm (°C)
YTH^YTHDF2 52.74
DMSO 52.72 -0.02
6 μM D-6 52.76 0.02
50 μM D-6 52.76 0.02
Tm (°C) ΔTm (°C)
YTH^YTHDF2 52.75
DMSO 52.71 -0.04
6 μM D-6 52.71 -0.04
50 μM D-6 52.75 0
Tm (°C) ΔTm (°C)
YTH^YTHDF2 52.79
DMSO 52.81 0.02
6 μM D-6 52.79 0
50 μM D-6 52.80 0.01
Fluorescence (normalizazion)
Temperature (°C)
C
Tm (°C) ΔTm (°C)
YTH^YTHDF3 58.17
DMSO 58.19 0.02
6 μM D-6 58.16 -0.01
50 μM D-6 58.17 0
Tm (°C) ΔTm (°C)
YTH^YTHDF3 58.10
DMSO 58.12 0.02
6 μM D-6 58.13 0.03
50 μM D-6 58.11 0.01
Tm (°C) ΔTm (°C)
YTH^YTHDF3 58.15
DMSO 58.17 0.02
6 μM D-6 58.14 -0.01
50 μM D-6 58.17 0.02
Fluorescence (normalizazion)
Temperature (°C)

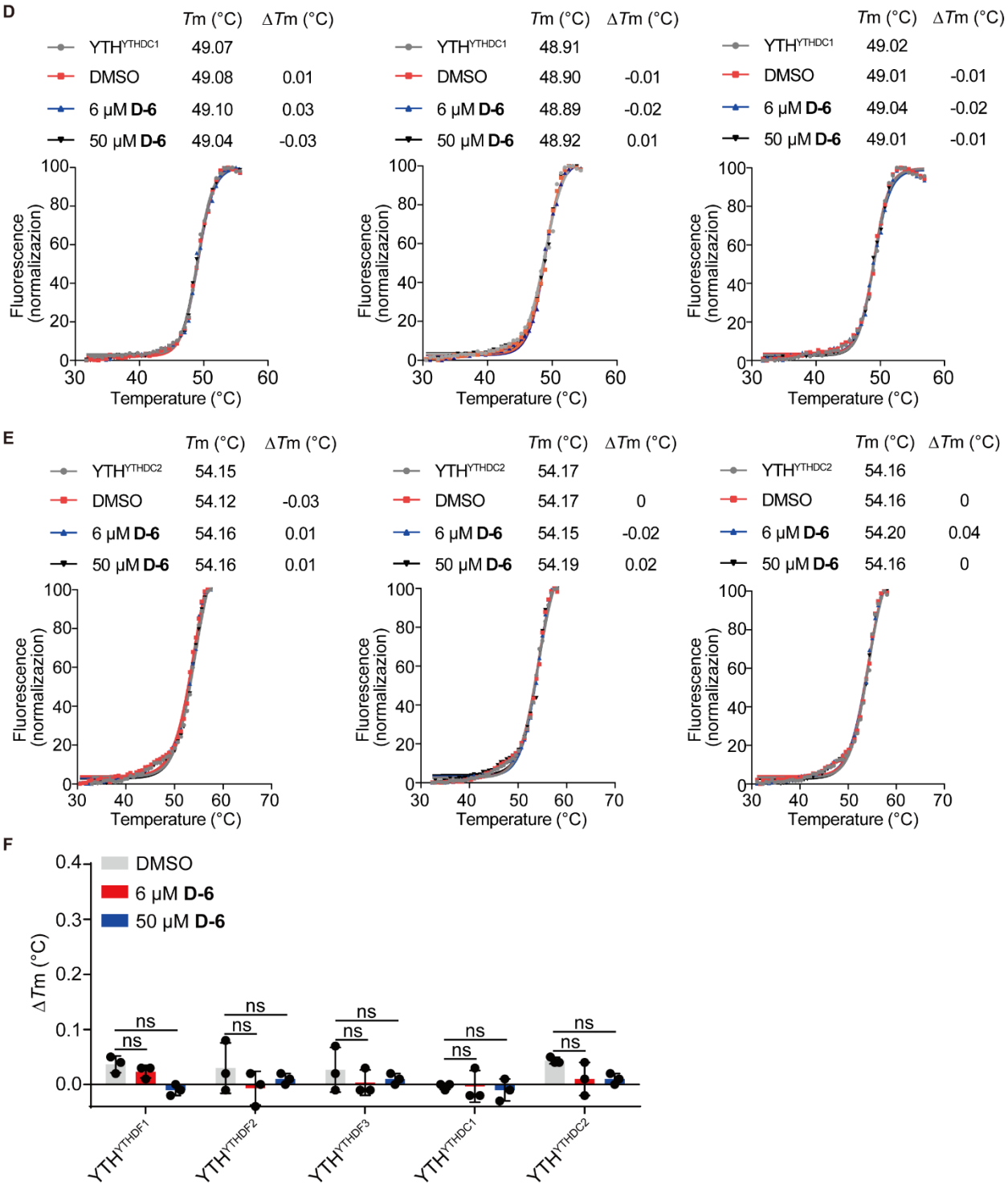

Fig. S15. Thermal shift assays results for no stabilization effect of the negative control compound D-6 against five YTH-domain proteins, including YTH^{YTHDF1} (A),

YTH^{YTHDF2} (B), YTH^{YTHDF3} (C), YTH^{YTHDC1} (D), and YTH^{YTHDC2} (E). Shown in (F) is the summary of ΔTm of different YTH domains by adding the D-6 compound.

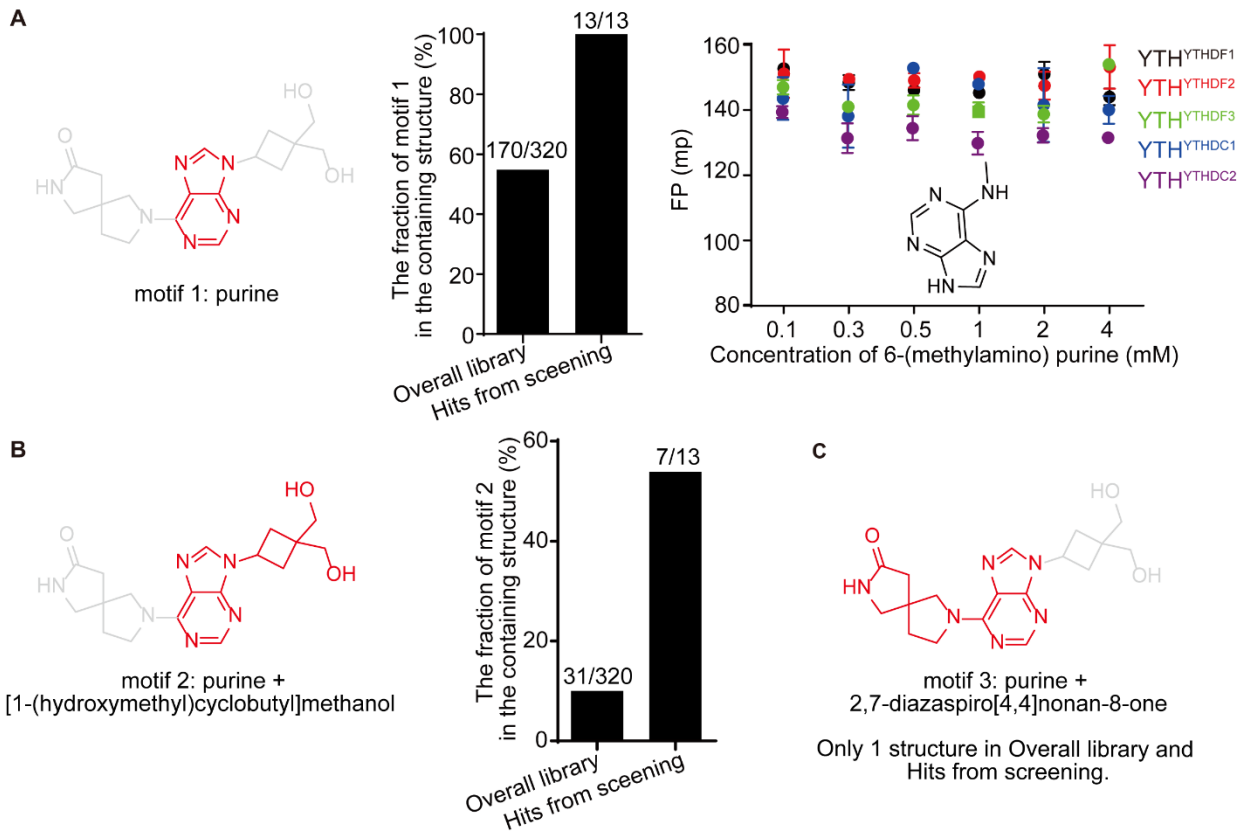

Fig. S16. Motif enrichment analysis of structural motifs in N-7. (**A**) The chemical structure of Motif 1 (colored in red) is shown on the left. The middle bar graph shows the fractions of compounds that contain Motif 1 out of all compounds in the overall library and in the hits from the screening in this study. The numbers of compounds are noted above the bar. Shown on the right are the dose-response curves for the 6-(methylamino) purine against YTH domain-m^{6}A recognition, measured by the FP competition assay. (**B**) Chemical structure of Motif 2 (colored in red) is shown on the left. The bar graph shows the fractions of compounds that contain Motif 2 out of the overall library and in the hits from the screening. (**C**) Shown is the chemical structure of Motif 3 (colored in red) and only one structure (**N-7**) contains Motif 3 in the overall library.

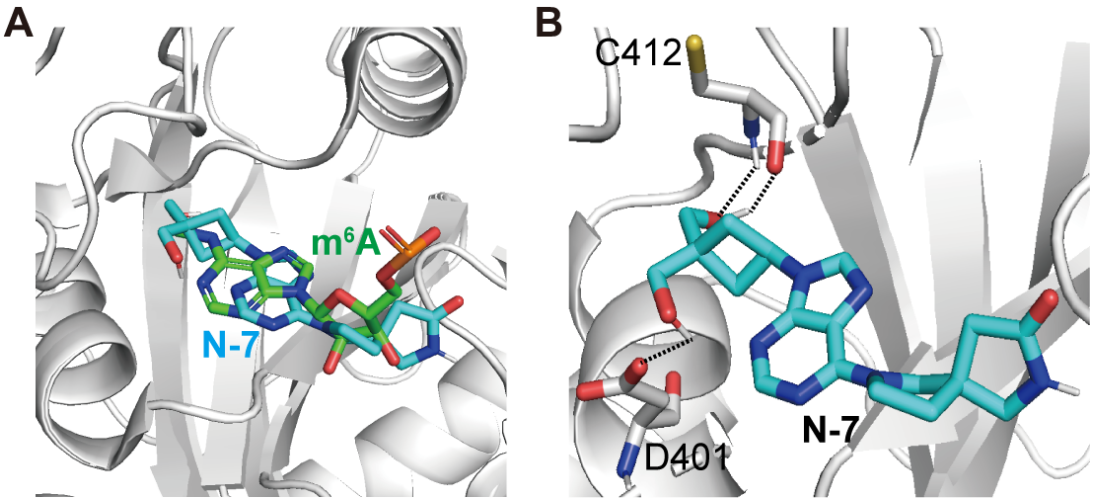

Fig. S17. Molecular Docking of N-7 and the YTH^{YTHDF1}. (**A**) Superimposition of the crystal structure of YTH^{YTHDF1}/m^{6}A (PDB: 4RCJ) and the best-ranked docking result of YTH^{YTHDF1} in complex with **N-7**. (**B**) Interactions between YTH^{YTHDF1} and **N-7** by docking. m^{6}A and **N-7** are represented by green and cyan sticks, respectively.

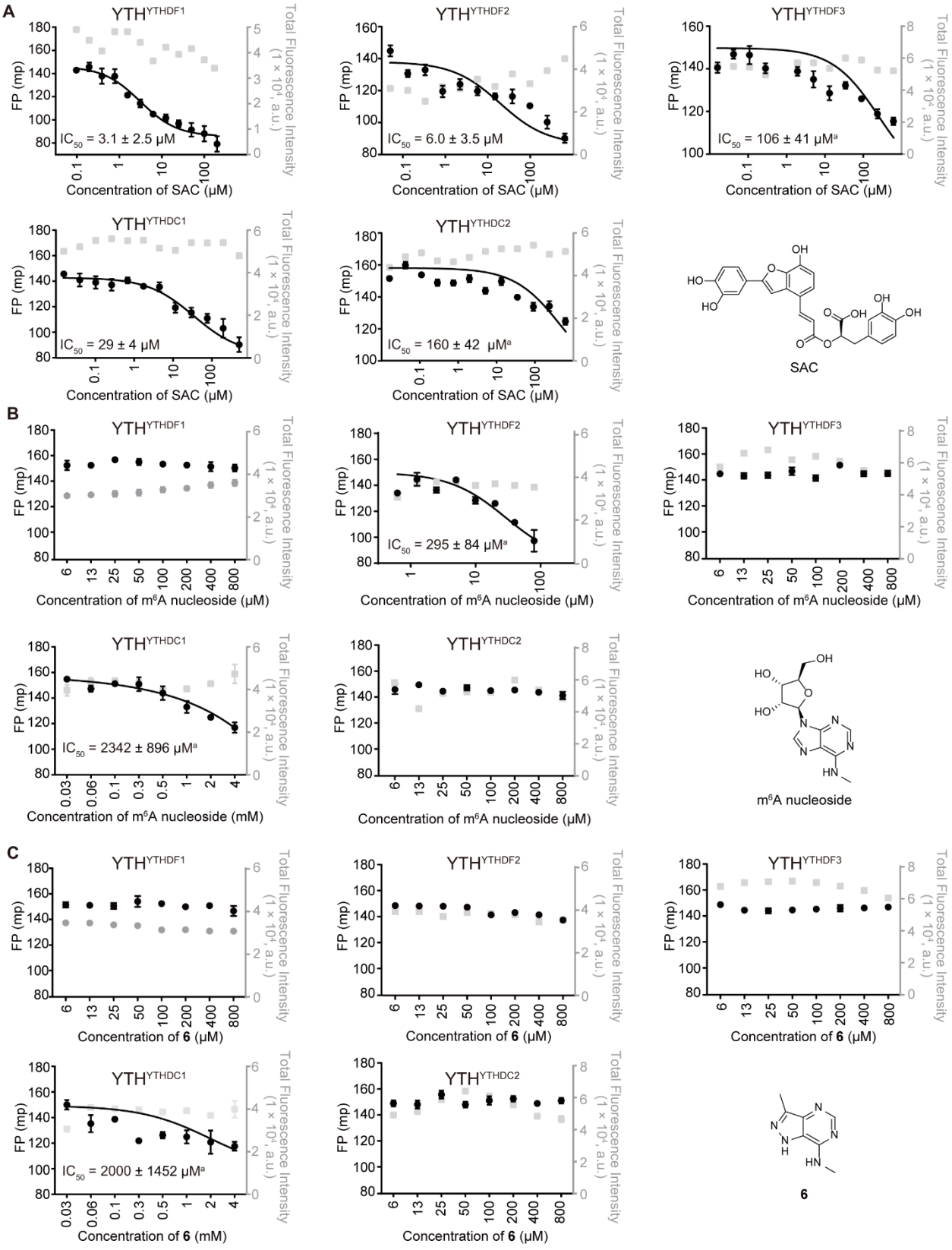
A
YTH^YTHDF1
YTH^YTHDF2
YTH^YTHDF3
YTH^YTHDC1
YTH^YTHDC2
FP (mp)
Total Fluorescence Intensity (1 × 10^4, a.u.)
IC50 = 3.1 ± 2.5 μM
IC50 = 6.0 ± 3.5 μM
IC50 = 106 ± 41 μM[a]
IC50 = 29 ± 4 μM
IC50 = 160 ± 42 μM[a]
Concentration of SAC (μM)
SAC
B
IC50 = 295 ± 84 μM[a]
IC50 = 2342 ± 896 μM[a]
Concentration of m6A nucleoside (μM)
Concentration of m6A nucleoside (mM)
m6A nucleoside
C
IC50 = 2000 ± 1452 μM[a]
Concentration of 6 (μM)
Concentration of 6 (mM)
6

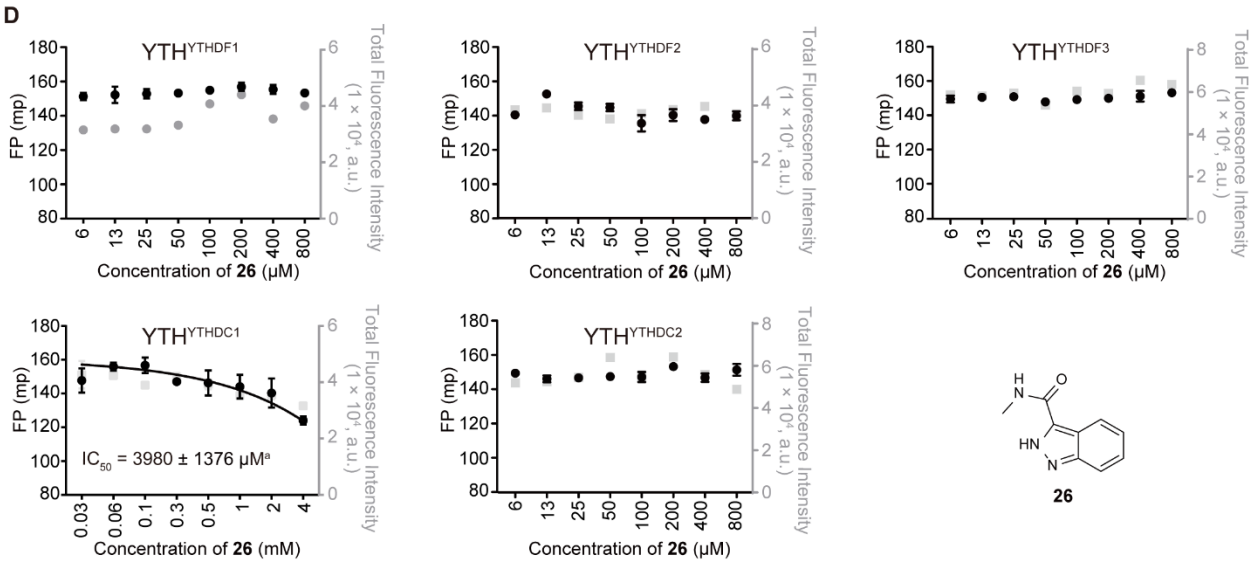

[a] We set the bottom value to 80 and the top value to 150 in GraphPad Prism for the log(inhibitor) vs. response (three parameters) analysis, as the compound did not completely decrease the FP at the highest concentration.

Fig. S18. FP competition assay using reported YTH domain inhibitors against all YTH domain proteins and FAM-m^{6}A-RNA. No visible aggregates were observed for the compounds under the assay concentration conditions. Data are presented as mean ± SD with n=2 or 3 biological replicates.

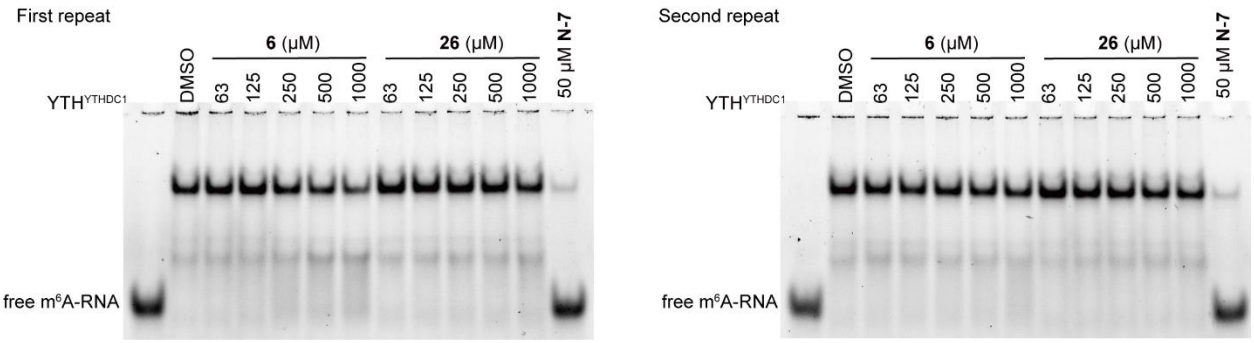

Fig. S19. Compounds 6 and 26 show minimal inhibition of the formation of the YTH^{YTHDC1} protein-RNA complex by the REMSA assay. No visible aggregates were observed for compounds **6** and **26** under the assay concentration conditions.